Title

Metabolic and thermal stimuli control K2P2.1 (TREK-1) through modular sensory and gating domains

Journal

The EMBO Journal, 31(15)

ISSN

0261-4189

Authors

Bagriantsev, Sviatoslav N
Clark, Kimberly A
Minor, Daniel L

Publication Date

2012-08-01

DOI

10.1038/emboj.2012.171

Peer reviewed

The EMBO Journal (2012) 31, 3297–3308 | © 2012 European Molecular Biology Organization | Some Rights Reserved 0261-4189/12
www.embojournal.org

THE EMBO JOURNAL

EMBO open

Metabolic and thermal stimuli control $K_{2P}2.1$ (TREK-1) through modular sensory and gating domains

Sviatoslav N Bagriantsev[1], Kimberly A Clark[1] and Daniel L Minor Jr[1,2,3,4,*]

[1]Cardiovascular Research Institute, University of California, San Francisco, CA, USA, [2]Department of Biochemistry and Biophysics, and Cellular and Molecular Pharmacology, Cardiovascular Research Institute, University of California, San Francisco, CA, USA, [3]California Institute for Quantitative Biomedical Research, University of California, San Francisco, CA, USA and [4]Physical Biosciences Division, Lawrence Berkeley National Laboratory, Berkeley, CA, USA

$K_{2P}2.1$ (TREK-1) is a polymodal two-pore domain leak potassium channel that responds to external pH, GPCR-mediated phosphorylation signals, and temperature through the action of distinct sensors within the channel. How the various intracellular and extracellular sensory elements control channel function remains unresolved. Here, we show that the $K_{2P}2.1$ (TREK-1) intracellular C-terminal tail (Ct), a major sensory element of the channel, perceives metabolic and thermal commands and relays them to the extracellular C-type gate through transmembrane helix M4 and pore helix 1. By decoupling Ct from the pore-forming core, we further demonstrate that Ct is the primary heat-sensing element of the channel, whereas, in contrast, the pore domain lacks robust temperature sensitivity. Together, our findings outline a mechanism for signal transduction within $K_{2P}2.1$ (TREK-1) in which there is a clear crosstalk between the C-type gate and intracellular Ct domain. In addition, our findings support the general notion of the existence of modular temperature-sensing domains in temperature-sensitive ion channels. This marked distinction between gating and sensory elements suggests a general design principle that may underlie the function of a variety of temperature-sensitive channels.

The EMBO Journal (2012) **31,** 3297–3308. doi:10.1038/emboj.2012.171; Published online 22 June 2012
Subject Categories: membranes & transport
Keywords: C-type gate; K_{2P} channel; leak current; potassium channel; temperature gating

Introduction

K_{2P} potassium channels generate a 'leak' or 'background' current that is important for the regulation of excitability in neurons, secretory cells, and cardiomyocytes (Enyedi and Czirjak, 2010). $K_{2P}2.1$ (*KCNK2*/TREK-1) (Fink *et al*, 1996), one of the best studied K_{2P}s, is expressed in nociceptive neurons (Talley *et al*, 2001; Alloui *et al*, 2006; Yamamoto *et al*, 2009) and contributes to sensitivity to inflammatory pain (Alloui *et al*, 2006), heat, and mechanical force (Noel *et al*, 2009). Importantly, the biophysical responses of $K_{2P}2.1$ (TREK-1), which is a polymodal ion channel controlled by extracellular pH (Cohen *et al*, 2008), temperature (Maingret *et al*, 2000), mechanical force (Patel *et al*, 1998), and a number of other stimuli (Noel *et al*, 2011), are well correlated with the categories of biological sensory processes associated with the channel. Thus, the fundamental responses of the channel appear to be directly linked to biological function.

The factors that modulate $K_{2P}2.1$ (TREK-1) activity have diverse physical natures, ranging from protons, to covalent modification by phosphorylation, to temperature. To detect these varied signals, the channel uses a gating apparatus that integrates commands from sensors located in different channel regions. There are two pH sensors that are located on opposite sides of the membrane, a P1 loop histidine that responds to extracellular pH (Cohen *et al*, 2008; Sandoz *et al*, 2009) and a glutamate on the intracellular C-terminal tail (Ct) (Honore *et al*, 2002), which is a major regulatory domain of the channel (Noel *et al*, 2011). Ct is the site of action for regulation by phospholipids (Chemin *et al*, 2005, 2007; Lopes *et al*, 2005), regulatory proteins (Sandoz *et al*, 2006, 2008), and phosphorylation (Patel *et al*, 1998; Murbartian *et al*, 2005). Further, deletion of Ct has been shown to abolish both thermosensitivity (Maingret *et al*, 2000) and mechanosensitivity (Patel *et al*, 1998). How these diverse sensors and factors control channel function has remained an important unanswered question.

Recent studies indicate that a number of the different $K_{2P}2.1$ (TREK-1) modulatory inputs sensed on either side of the membrane converge on an extracellular C-type gate (Bagriantsev *et al*, 2011) that involves the selectivity filter. This gate has been shown to respond to extracellular pH (Cohen *et al*, 2008; Sandoz *et al*, 2009; Bagriantsev *et al*, 2011; Ma *et al*, 2011), intracellular pH (Piechotta *et al*, 2011), temperature (Bagriantsev *et al*, 2011), and mechanical force (Bagriantsev *et al*, 2011). Although three of these responses involve Ct, it has been unknown whether other factors that act on Ct, such as phospholipids and phosphorylation, also act via the $K_{2P}2.1$ (TREK-1) C-type gate. Moreover, it has remained unclear how the different regulatory cues that act on Ct translate into gating commands. Previous models have proposed that association of the $K_{2P}2.1$ (TREK-1) Ct with the negatively charged phospholipids in the plasma membrane leads to channel activation (Chemin *et al*, 2005), whereas the converse inhibits the channel (Honore *et al*, 2002; Chemin *et al*, 2005, 2007; Lopes *et al*, 2005; Sandoz *et al*, 2011). Nevertheless, how such changes might impact the C-type gate has not been tested and whether there is crosstalk between the intracellular and extracellular responses is unknown.

*Corresponding author. Department of Biochemistry and Biophysics, and Cellular and Molecular Pharmacology, Cardiovascular Research Institute, University of California, San Francisco, CA 94158-2330, USA. Tel.: +1 415 514 2551; Fax: +1 415 514 2550;
E-mail: daniel.minor@ucsf.edu

Received: 18 April 2012; accepted: 25 May 2012; published online: 22 June 2012

Here, by examining mutations in the context of both homodimeric channels and hetrodimeric concatemers, we show that Ct influences K_{2P}2.1 (TREK-1) activity by acting on the extracellular C-type gate and that there is clear cross-talk between the status of the C-type gate and Ct. Further, we demonstrate that Ct, not the gate, is the primary heat-sensing element of the channel. The data lead to a model in which Ct affects conformational changes directly within its own subunit via M4 and the first pore helix, pore helix 1 (PH1). The distinct segregation between the temperature sensor and the gate may have general implications for how diverse types of temperature-sensitive channels function.

Results

Intracellular C-terminal domain (Ct) regulates K_{2P}2.1 (TREK-1) activity at the extracellular C-type gate

In search of a general paradigm in which we could test how the intracellular Ct modulates K_{2P}2.1 (TREK-1), we examined the response of mouse K_{2P}2.1 (TREK-1) to regulation by membrane potential changes. Similar to observations with human K_{2P}2.1 (TREK-1) (Segal-Hayoun *et al*, 2010), we found that mouse K_{2P}2.1 (TREK-1) expressed in *Xenopus laevis* oocytes exhibited membrane potential-dependent activity changes that occurred on the minute timescale (Figure 1A and Supplementary Figure S1). Clamping the membrane potential at 0 mV for four minutes in a physiological buffer (2 mM external potassium, pH 7.4) caused gradual loss of K_{2P}2.1 (TREK-1) current that could be reversed upon prolonged hyperpolarization to −100 mV (Figure 1A and Supplementary Figure S1). Prolonged membrane potential changes trigger a G_q-protein-coupled receptor (G_qPCR) cascade in *Xenopus laevis* oocytes that activates kinases (Cohen and Zilberberg, 2006) and phospholipases (Segal-Hayoun *et al*, 2010), factors that affect K_{2P}2.1 (TREK-1) function through Ct in both amphibian (Segal-Hayoun *et al*, 2010) and mammalian (Chemin *et al*, 2005; Lopes *et al*, 2005; Murbartian *et al*, 2005) systems. In line with this mechanism, we found that mouse K_{2P}2.1 (TREK-1) carrying a mutation in Ct at a key phosphorylation site, S300A (Murbartian *et al*, 2005) (Figure 1B), displayed decreased sensitivity to membrane potential changes (Figure 1C–E). This result is consistent with prior studies of the homologous S315A mutation in human K_{2P}2.1 (TREK-1) (Segal-Hayoun *et al*, 2010). Thus, monitoring regulation of mouse K_{2P}2.1 (TREK-1) by changes in membrane potential presented a facile tool to assay regulation of channel activity by multiple commands converging on Ct.

A number of modalities that rely on Ct to control K_{2P}2.1 (TREK-1) function (Patel *et al*, 1998; Maingret *et al*, 2000; Honore *et al*, 2002) act on the extracellular C-type gate (Bagriantsev *et al*, 2011; Piechotta *et al*, 2011). This gate can be stabilized by high concentrations of extracellular potassium, $[K^+]_o$ (Cohen *et al*, 2008; Bagriantsev *et al*, 2011), a manipulation that blunts the response to the control input. To see whether the membrane potential-driven, Ct-mediated changes in K_{2P}2.1 (TREK-1) activity have a similar sensitivity to $[K^+]_o$, we compared the influence of membrane potential on K_{2P}2.1 (TREK-1) activity in 2 and 90 mM $[K^+]_o$ (Figure 1D–F). Indeed, elevated $[K^+]_o$ greatly reduced the response to membrane potential changes. These findings suggest a general involvement of the C-type gate in K_{2P}2.1 (TREK-1) activation by Ct, regardless of the modality used to control the channel and lead us to search for the mechanism that connects the action of Ct to the C-type gate.

A key position in PH1 affects C-type gating

In other potassium channel classes, selectivity filter conformation and function, which comprises the core of the C-type gate, is coupled to structural features in the pore helix (Yang *et al*, 1997; Alagem *et al*, 2003; Cordero-Morales *et al*, 2006; Tao *et al*, 2009; Cheng *et al*, 2011; Cordero-Morales *et al*, 2011b). Given the probable general importance of pore helix-selectivity filter interactions for potassium channel function, we sought evidence for a role for the pore helix in K_{2P}2.1 (TREK-1) gating. Sequence alignment of the PH1 segment from diverse K_{2P}s pointed to the K_{2P}2.1 (TREK-1) Gly137 position as one of the few variable residues in this region (Figure 2A and Supplementary Figure S2). Notably, in two K_{2P} channels from the TASK group, K_{2P}3.1 (*KCNK3*/TASK-1) and K_{2P}9.1 (*KCNK9*/TASK-3), the Gly137 equivalent position has the much larger, β-branched alkyl sidechain amino-acid isoleucine.

Given the large volume difference between these sidechains (106 Å^3), we made the G137I K_{2P}2.1 (TREK-1) mutant and examined the response to inhibition by extracellular acidosis (pH_o), a readily accessible assay of C-type gate stability in K_{2P}2.1 (TREK-1) (Cohen *et al*, 2008; Bagriantsev *et al*, 2011) and other K_{2P}s (Lopes *et al*, 2000; Clarke *et al*, 2008; Niemeyer *et al*, 2010). Remarkably, G137I caused K_{2P}2.1 (TREK-1) to be exceptionally resistant to pH_o inhibition (Figure 2B–D, Table I). The G137I change also prevented the apparent change in relative ion permeability from potassium to sodium that associated with C-type channel closure (Cohen *et al*, 2008; Bagriantsev *et al*, 2011) (Supplementary Figure S3A–C). Together, both effects indicate that the G137I mutation stabilized the C-type gate. Conversely, the reciprocal I88G change in PH1 of both K_{2P}3.1 (TASK-1) and K_{2P}9.1 (TASK-3) potentiated inhibition by low pH_o (Figure 2E–J and Table I). Thus, the data strongly support a critical role for PH1 in K_{2P} selectivity filter gating.

Stabilization of the C-type gate blunts channel modulation by Ct

Previous investigation (Bagriantsev *et al*, 2011) identified a crucial residue in the N-terminal portion of the M4 transmembrane segment, Trp275 (Figure 1B), where changes to nonaromatic residues antagonize pH_o inhibition, temperature and stretch activation, and stabilize the C-type gate in an active, potassium-selective conformation. Having identified mutations in two elements involved in C-type gate stabilization, PH1 and M4, we next asked whether either influenced channel modulation by Ct. Indeed, both the PH1 helix G137I mutant and the M4 W275S mutant caused a marked reduction in the ability of membrane potential to affect channel function (Figure 3A–D). Recent determination of the 3.8Å resolution structure of K_{2P}4.1 (*KCNK4*/TRAAK) (Brohawn *et al*, 2012), which is closely related to K_{2P}2.1 (TREK-1), shows that the equivalent PH1 and M4 positions (Gly124 and Trp262) contact each other and, thus, provides a clear rationalization for how changes in sidechain volume at either position can impact the pore (Figure 3E). The location of these residues together with the common effects that the

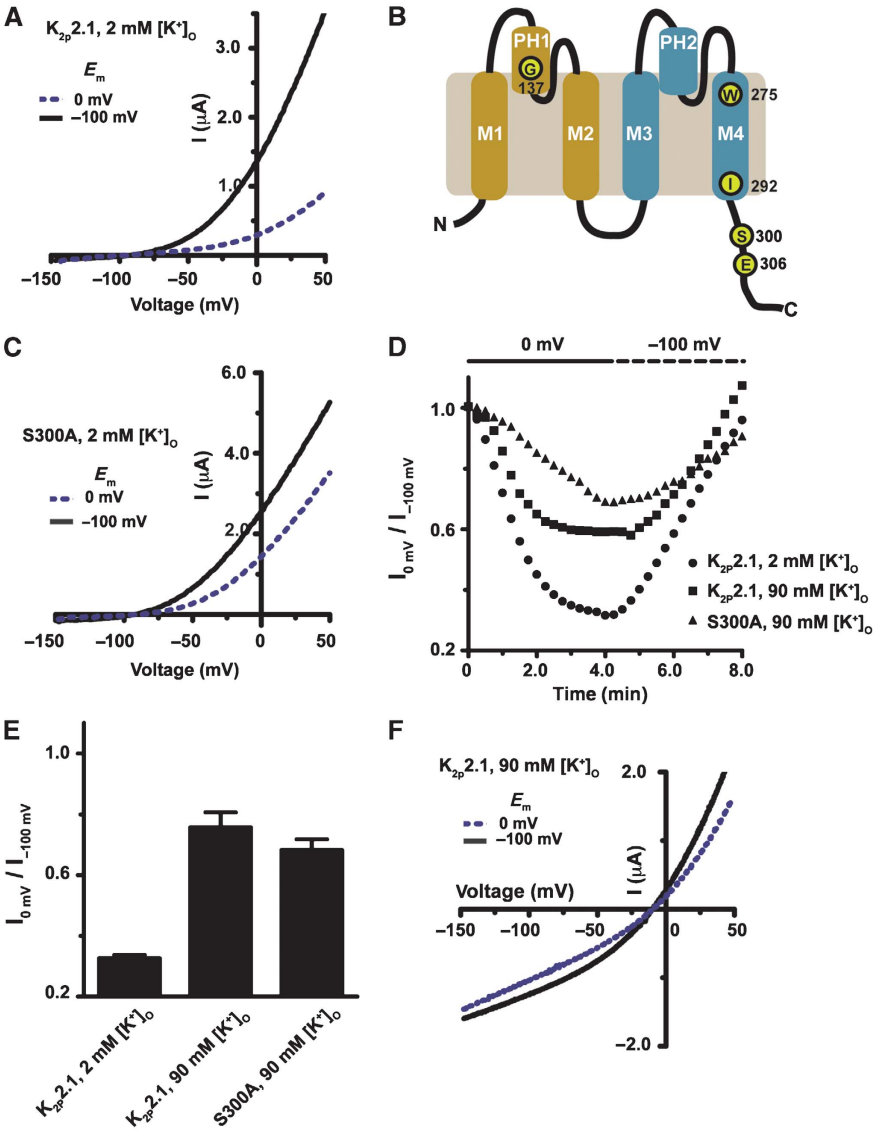

Figure 1 Extracellular potassium antagonizes regulation of $K_{2P}2.1$ (TREK-1) by membrane potential. (**A**) Effect of membrane potential (E_M) on $K_{2P}2.1$ (TREK-1) activity in *Xenopus laevis* oocytes measured by two-electrode voltage clamp in 2 mM $[K^+]_o$ pH 7.4. Current–voltage (*I-V*) curves show exemplar voltage-clamp recordings of $K_{2P}2.1$ (TREK-1) activity after 4 min of holding at −100 and 0 mV, consecutively. (**B**) Cartoon diagram of a single $K_{2P}2.1$ (TREK-1) subunit, transmembrane segments 1–4 (M1–M4), pore helix 1 and pore helix 2 (PH1, PH2), and the positions of key residues are indicated. (**C**) Exemplar I–V curves showing the effect of E_M on $K_{2P}2.1$ (TREK-1) S300A. (**D**) Channel activity from a representative cell in response to changes in E_M. Channel activity was assayed every 15 s by a ramp from −150 to 50 mV. Following current stabilization at −100 mV, E_M was changed to 0 mV, and channel activity was assayed by the ramp protocol until current reached minimal values (usually within 4–5 min). Channel activity was reversed by returning E_M to −100 mV. Each point represents channel activity from the ramp curves at 0 or +50 mV for 2 mM and 90 $[K^+]_o$ solutions, respectively. Data presented as fraction relative to activity after initial stabilization at −100 mV. (**E**) Quantification of maximal inhibition of WT or mutant $K_{2P}2.1$ (TREK-1) by prolonged incubation at 0 mV (mean ± s.e., $n \geqslant 6$, $N \geqslant 2$, where '*n*' is the number of oocytes and '*N*' in the number of independent oocyte batches). (**F**) I–V curves showing exemplar voltage-clamp recordings of $K_{2P}2.1$ (TREK-1) in 90 mM $[K^+]_o$ pH 7.4 after stabilization at, consecutively, −100 and 0 mV.

pore-stabilizing mutations at these positions have on Ct-based regulatory signals suggested that Ct action directly affects the C-type gate. Given that Ct and the C-type gate are on opposite sides of the channel relative to the bilayer (Figure 1B), we next sought to define the mechanism that might mediate communication between these components.

Transmembrane helix 4 mediates communication between Ct and the C-type gate

Our leading hypothesis for communication between Ct and the C-type gate was transduction through M4 as this component is covalently linked to Ct and bears an essential element of the gate, Trp275 (Bagriantsev *et al*, 2011). Following strategies employed previously for uncoupling the effects of intracellular domains from voltage-gated calcium channel pores (Arias *et al*, 2005; Zhang *et al*, 2008; Findeisen and Minor, 2009), we substituted three residues at the predicted M4–Ct junction, Ile292-Gly293-Asp294, with glycines to introduce flexibility, $K_{2P}2.1$-3G, or alanines, $K_{2P}2.1$-3A, to remove sidechain interactions (Figure 4A). Both substitutions rendered the resulting mutant channels insensitive to inhibitory (0 mV) and activating (−100 mV) membrane potentials (Figure 4B and C), indicating that both changes eliminated the influence of Ct on function. Importantly, these mutants

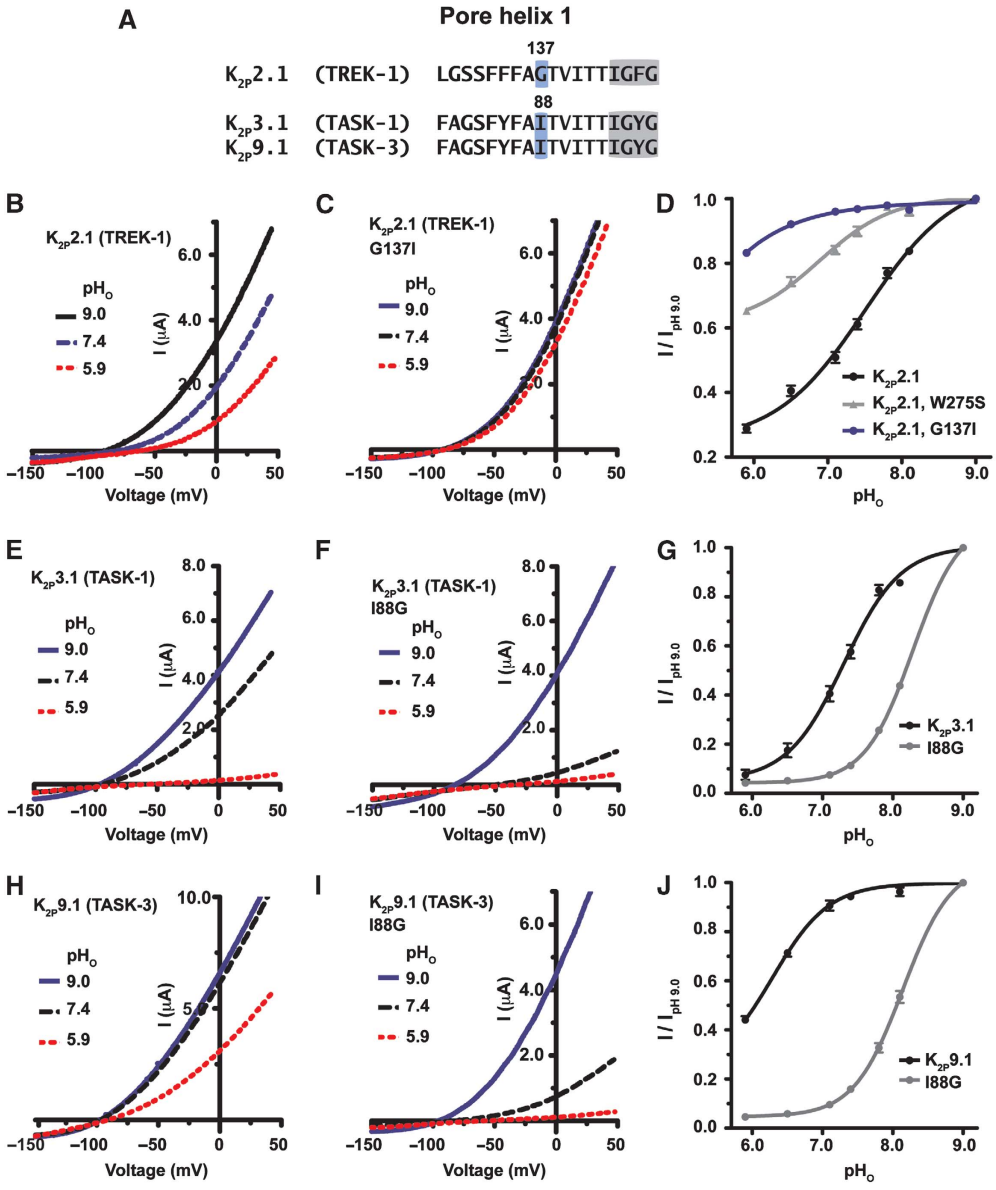

Figure 2 PH1 is critical for K_{2P} channels C-type gating. (**A**) Amino-acid alignment of the PH1 region of the indicated K_{2P} channels. The GXG selectivity filter sequence is highlighted in grey. (**B, C, E, F, H, I**) Exemplar recordings of the response of the indicated K_{2P} channels to the external pH (pH_o) changes in 2 mM $[K^+]_o$ solution. Currents were elicited by a voltage ramp from -150 to $+50$ mV, from a holding potential of -80 mV. (**D, G, J**) Quantitation of the response of the K_{2P} channels to changes in pH_o. Data (mean ± s.e., $n \geqslant 6$, $N \geqslant 2$) was taken at 0 mV, normalized to activity at pH 9.0, and fitted to the Hill equation.

retained sensitivity to pH_o inhibition (Figure 4D) and support the idea that the absence of responses to membrane potential changes was not caused by malfunctioning C-type gate, but rather due to uncoupling of Ct from the pore. This notion was further strengthened by the observation that both changes made the channel more sensitive to pH_o inhibition (IC_{50}, mean ± s.e., 7.90 ± 0.03 and 7.91 ± 0.08 versus 7.51 ± 0.05 for K_{2P}2.1-3G, K_{2P}2.1-3A, and K_{2P}2.1, respectively, Table I; $P = 0.0003$ and 0.003, *t*-test, for K_{2P}2.1-3G and K_{2P}2.1-3A, versus K_{2P}2.1, respectively), a result that suggests the loss of some degree of tonic activation from Ct.

To test coupling between Ct and the C-type gate further, we turned our attention to the previously characterized activating mutant located in Ct, E306A (Honore *et al*, 2002), that is thought to activate the channel by increasing interactions between Ct and the membrane inner leaflet (Chemin *et al*, 2005; Sandoz *et al*, 2011). Similar to the activating effects of mutations in the C-type gate (Figure 3D), we found that E306A decreased sensitivity of K_{2P}2.1 (TREK-1) to pH_o inhibition (pH_o $IC_{50} = 7.19 \pm 0.09$) (Figure 4E, Supplementary Figure S4B and Table I). This effect was eliminated when E306A was placed in the context of K_{2P}2.1-3G (Figure 4F and Table I). Indeed, similar to K_{2P}2.1-3G alone, the K_{2P}2.1-3G/E306A channel was more sensitive to pH_o gating than wild-type (pH_o IC_{50} mean ± s.e., 7.83 ± 0.01 versus 7.90 ± 0.03, $P = 0.07$, 3G/E306A and K_{2P}2.1-3G, respectively). Taken together, our data strongly suggest that Ct affects K_{2P}2.1 (TREK-1) by acting through the M4 segment to control the extracellular C-type gate and show that there is substantial crosstalk between Ct and the C-type gate.

Ct affects the gate through cis-interactions with M4

$K_{2P}2.1$ (TREK-1) channels are composed of two identical subunits that each bear a single Ct. Given the evidence that Ct affects channel activity by coupling through M4 to the extracellular C-type gate, we next asked whether the Ct acts by a *cis*-type mechanism involving M4 of the same subunit or *trans*-type mechanism involving M4 of the neighbouring subunit. To test this, we constructed a tandem channel in which the wild-type (WT) subunits were connected by 20-residue flexible linker having the sequence $(Ala)_3$-$(Gly\text{-}Ser\text{-}Gly)_3$-$(Gly\text{-}Ser\text{-}Ser)_2$–Gly–Ser. To establish that the tandem channels are properly made, we compared N-terminal hemagglutinin (HA) tagged wild-type and tandem $K_{2P}2.1$ (TREK-1) channels expressed in *Xenopus* oocytes by western blot analysis. WT $K_{2P}2.1$ (TREK-1) produced two bands that correspond to the approximate sizes of mature monomer (46.4 kDa) and dimer (92.8 kDa) (Figure 5A). In contrast, the tandem channel, WT–WT (93.1 kDa), migrated at a position matching the mobility of the dimer band from the nonlinked channel (Figure 5A). Treatment of the lysates with endoglycosydase H (EndoH) decreased the apparent molecular weight of the monomer and dimer and species by ~5 and 10 kDa, respectively, consistent with the prediction that each $K_{2P}2.1$ (TREK-1) monomer contains two *N*-linked glycosylation sites (Fink *et al*, 1996). Notably, we did not detect any low-molecular weight species in the WT–WT lysates. Therefore, the data indicate that the tandem dimers remain intact and the linker is not susceptible to appreciable proteolytic degradation.

Table I pH_o responses of K_{2P} channels and mutants

	Channel	pH_o IC_{50} ± s.e.[a]
$K_{2P}2.1$ (TREK-1)	$K_{2P}2.1$	7.51 ± 0.05
	G137I	ND
	W275S	6.89 ± 0.12
	3G	7.90 ± 0.03
	3A	7.91 ± 0.08
	E306A	7.19 ± 0.09
	3G/E306A	7.83 ± 0.01
$K_{2P}2.1$ (TREK-1) tandem	WT–WT	7.55 ± 0.04
	3G–3G	7.98 ± 0.07
	3G–WT	7.87 ± 0.04
	WT–3G	7.79 ± 0.02
	E306A–E306A	7.13 ± 0.04
	E306A-WT	7.30 ± 0.05
	E306A-3G	7.28 ± 0.05
	3G/E306A-WT	7.70 ± 0.03
	WT–3G/E306A	7.70 ± 0.03
$K_{2P}9.1$ (TASK-3)	$K_{2P}9.1$	6.29 ± 0.17
	I88G	8.21 ± 0.04
$K_{2P}3.1$ (TASK-1)	$K_{2P}3.1$	7.30 ± 0.04
	I88G	8.28 ± 0.03

ND, not determined.
[a]Data from fits to the Hill equation. $n \geqslant 6$, $N \geqslant 2$ for all constructs.

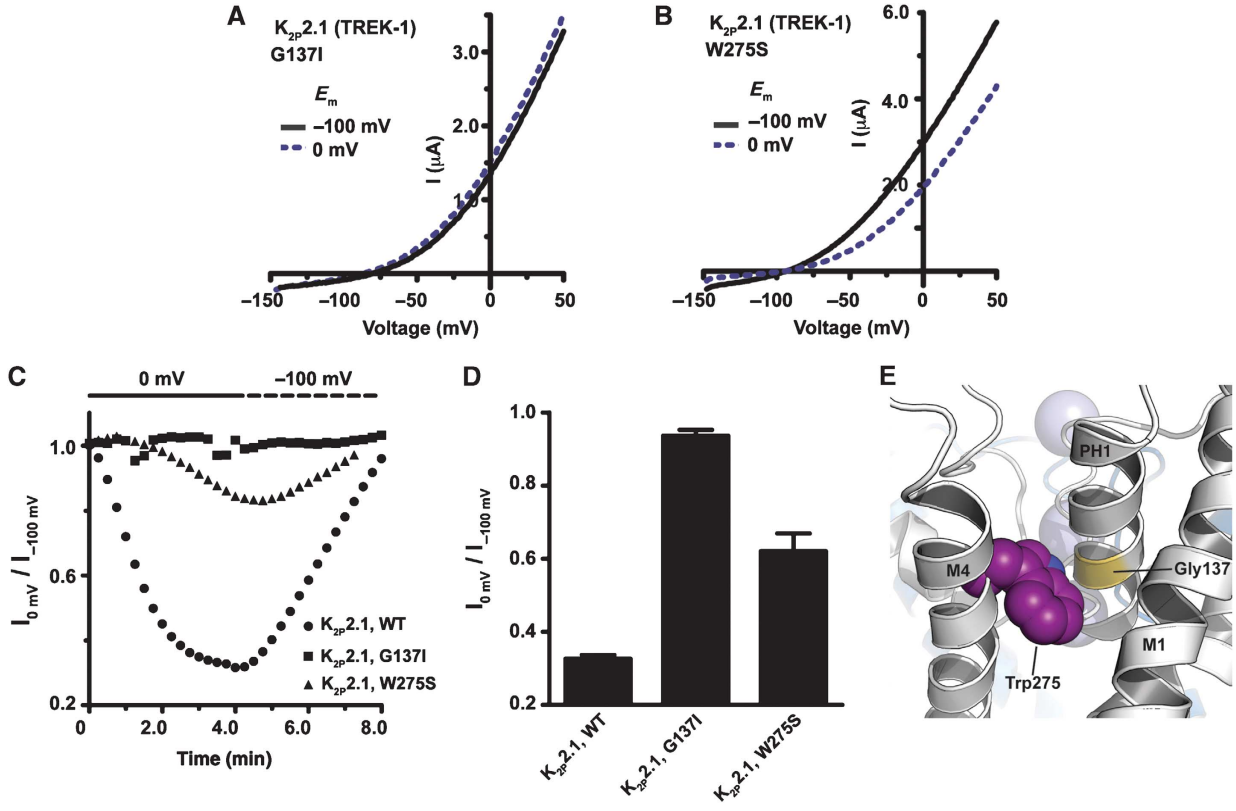

Figure 3 Mutations that stabilize the C-type gate antagonize regulation of $K_{2P}2.1$ (TREK-1) by membrane potential. (**A, B**) Exemplar recordings from oocytes expressing the indicated $K_{2P}2.1$ (TREK-1) mutants after prolonged incubation at, consecutively, −100 and 0 mV in 2 mM $[K^+]_o$ pH 7.4. After current stabilization at −100 mV, the membrane potential was changed to 0 mV, and the current was recorded every 15 s using a voltage ramp from −150 to +50 mV. (**C**) Exemplar time resolution of channel activity from a representative cell in response to fluctuating E_M in 2 mM $[K^+]_o$ pH 7.4. Each point represents channel activity from the ramp curves at 0 mV. Data presented as fraction relative to activity after initial stabilization at −100 mV. (**D**) Quantification of maximal $K_{2P}2.1$ (TREK-1) inhibition by prolonged incubation at 0 mV (mean ± s.e., $n \geqslant 6$, $N \geqslant 2$). (**E**) Ribbon diagram showing the location of Trp275 and Gly137 of $K_{2P}2.1$ (TREK-1) on the crystal structure of $K_{2P}4.1$ (TRAAK) (Brohawn *et al*, 2012)(PDB ID 3UM7). M4, transmembrane helix 4. PH1, pore helix 1. Blue spheres depict potassium ions.

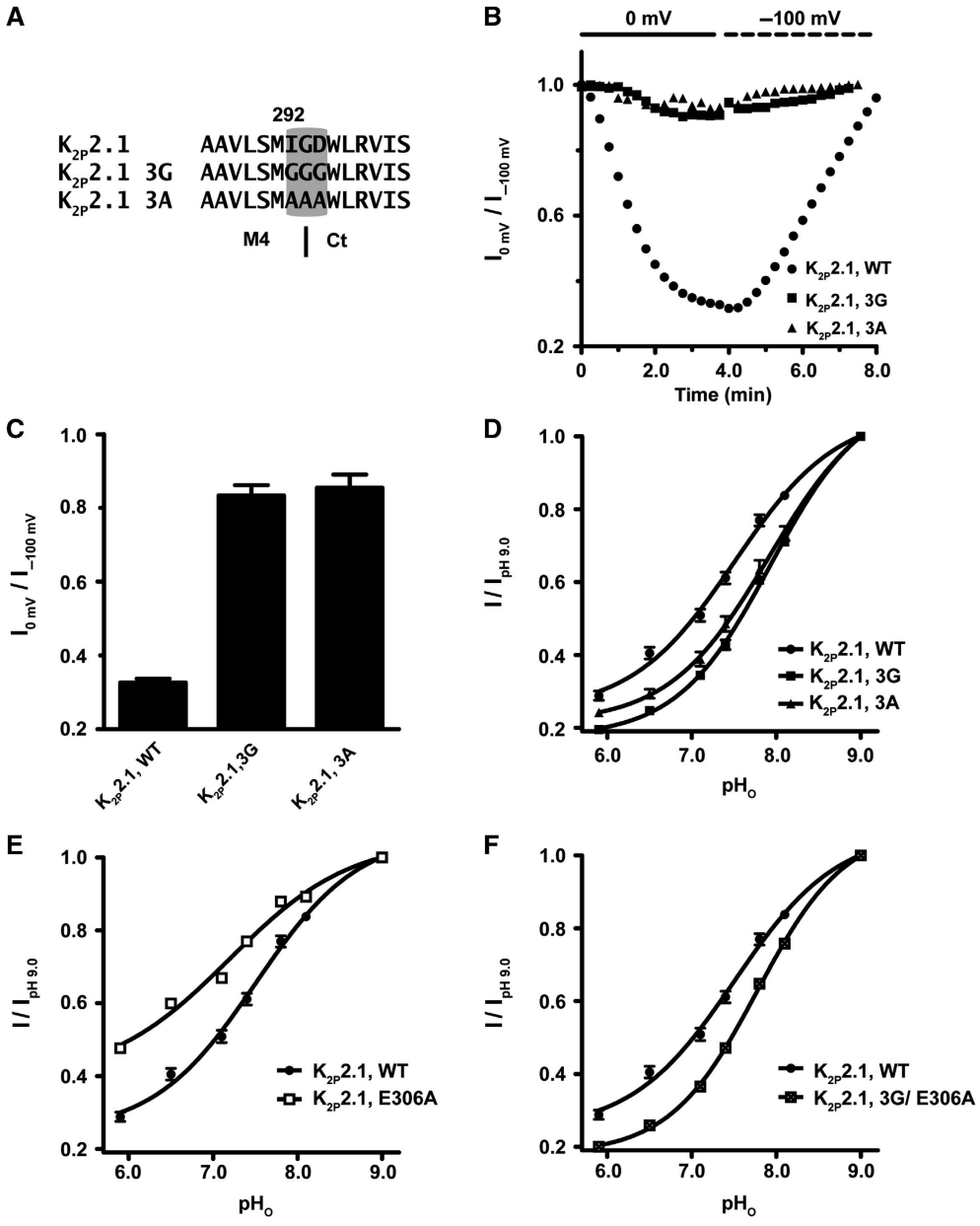

Figure 4 M4–Ct junction is critical for cross-talk between Ct and the C-type gate. (**A**) Amino-acid sequence of the M4–Ct junction region of $K_{2P}2.1$ (TREK-1) showing the location of the 3G and 3A mutations. Dashed line indicates a predicted boundary between M4 and Ct. (**B**) Exemplar time resolution of channel activity from a representative cell in response to fluctuating E_M in 2 mM $[K^+]_o$ pH_o 7.4. Each point represents channel activity from the ramp curves at 0 mV. Data presented as fraction relative to activity after initial stabilization at −100 mV. (**C**) Quantification of maximal $K_{2P}2.1$ (TREK-1) inhibition by prolonged incubation at 0 mV (mean ± s.e., $n \geqslant 6$, $N \geqslant 2$). (**D–F**) Normalized responses of the indicated channels to pH_o changes in 2 mM $[K^+]_o$. Currents were elicited by a voltage ramp from −150 to +50 mV, from a holding potential of −80 mV. Data (mean ± s.e., $n \geqslant 6$, $N \geqslant 2$) was taken at 0 mV, normalized to activity at pH 9.0 and fitted to the Hill equation.

We next characterized the functional properties of the tandem dimer. Electrophysiological measurements showed that the pH_o response of the tandem WT construct, WT–WT, was indistinguishable from WT $K_{2P}2.1$ (TREK-1) (pH_o $IC_{50} = 7.55 \pm 0.04$ and 7.51 ± 0.05, respectively, $P = 0.58$, *t*-test) (Figure 5B, Supplementary Figure S5A, and Table I). Ion selectivity was also unchanged (Supplementary Figure S5B). Furthermore, tandem $K_{2P}2.1$ (TREK-1) constructs bearing the triple glycine mutant (3G–3G) or the E306A mutant (E306A–E306A) in both subunits showed pH_o sensitivities that were not statistically different from those produced by the same mutations in the nontandem background (pH_o $IC_{50} = 7.98 \pm 0.07$ and 7.90 ± 0.03, $P = 0.19$, 3G–3G and $K_{2P}2.1$-3G, and 7.13 ± 0.04 versus 7.19 ± 0.09, $P = 0.58$, E306A-E306A and $K_{2P}2.1$-306A, respectively) (Figure 5B and Table I). These results provide strong evidence that the presence of the linker does not cause major functional perturbations and that the tandem constructs behave essentially the same as the nonlinked proteins. Thus, we used this background to assess the *cis*- versus *trans*- effects of Ct mutants.

Incorporation of the triple glycine change into only one subunit of the tandem shifted the pH_o response in the same direction as the corresponding double mutant (Figure 5C and Table I) and nontandem mutant; however, the magnitude of the effect was reduced (pH_o $IC_{50} = 7.87 \pm 0.04$, 7.79 ± 0.02,

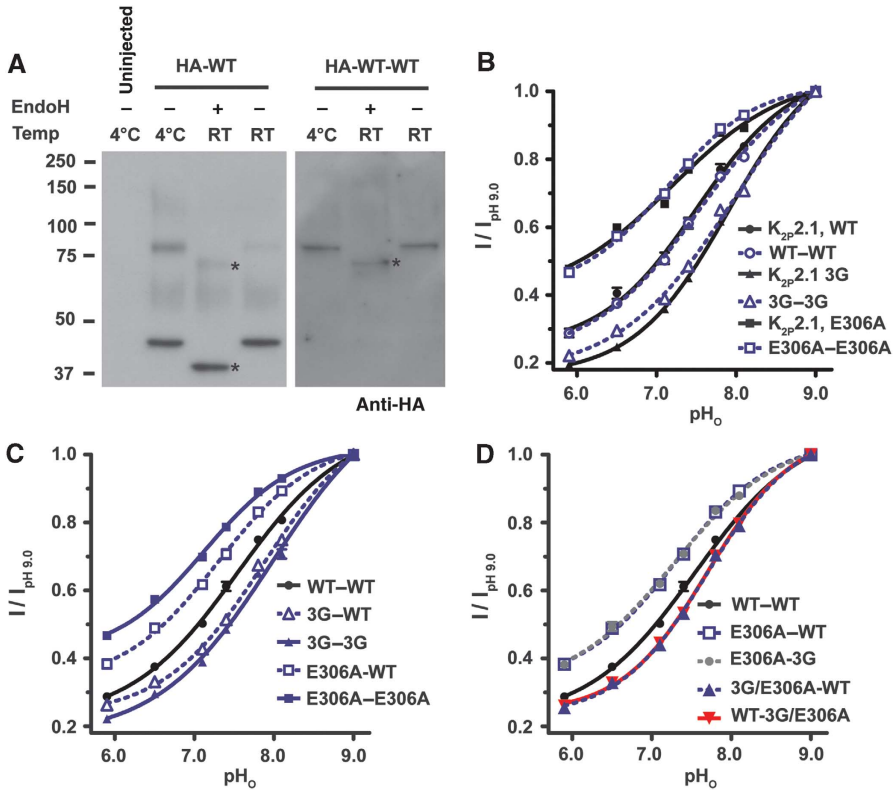

Figure 5 Ct domains act cooperatively to affect $K_{2P}2.1$ (TREK-1) function. (**A**) Immunoblot analysis of lysates from oocytes expressing HA-tagged WT, HA-WT or tandem HA-WT-WT $K_{2P}2.1$ (TREK-1) channels. Lysates were pre-incubated with or without EndoH for 1 h at 4°C or at room temperature (RT). Before electrophoresis, all samples were treated with 2% SDS and 2% β-mercaptoethanol for 15 min at 50°C to dissociate $K_{2P}2.1$ (TREK-1) subunits. Asterisks denote deglycolysated forms of WT and tandem channels. (**B–D**) Normalized responses of the indicated $K_{2P}2.1$ (TREK-1) channels to pH_o changes 2 mM $[K^+]_o$. Currents were elicited by a voltage ramp from −150 to +50 mV, from a holding potential of −80 mV. Data (mean ± s.e., $n \geqslant 6$, $N \geqslant 2$) was taken at 0 mV, normalized to activity at pH 9.0 and fitted to the Hill equation.

7.98 ± 0.07, and 7.93 ± 0.04 for 3G-WT, WT–3G, 3G-3G, and $K_{2P}2.1$-3G, respectively). Similarly, incorporation of a single E306A change into the tandem reduced the pH_o response but to a smaller extent than incorporation of the change into both subunits (pH_o IC_{50} = 7.30 ± 0.05, 7.13 ± 0.04, and 7.19 ± 0.09 for E306A-WT, E306A-E306A, and $K_{2P}2.1$-3G, respectively).

To test whether Ct acts on the C-type gate via a *cis*- or *trans*-mechanism, we analysed the pH_o responses of tandems that carry different combination of the triple glycine and E306A changes. The construct having E306A and 3G in separate tails (E306A-3G) showed a pH_o response that was not significantly different from that having only E306A in the first subunit of the tandem (Figure 5D and Table I) (pH_o IC_{50} = 7.28 ± 0.05 and 7.30 ± 0.05, P = 0.75, for E306A-3G and E306A-WT, respectively). In contrast, combination of the 3G and E306A mutations into the same Ct drastically abrogated the stabilizing effect of E306A (Figure 5D and Table I). This effect was independent of which tail bore the changes (pH_o IC_{50} = 7.70 ± 0.30 and 7.70 ± 0.30 for E306A/3G–WT and WT-E306A/3G, respectively). Thus, communication between Ct and the C-type gate occurs via *cis*-type mechanism.

Both Ct domains are required to achieve full temperature response of $K_{2P}2.1$ (TREK-1)

Having established that Ct acts through M4 of its own subunit, we finally turned our attention to $K_{2P}2.1$ (TREK-1) activation by temperature (Maingret *et al*, 2000) (Figure 6A), a response that depends on the C-type gate (Bagriantsev *et al*, 2011). Whether the C-type gate senses temperature changes directly, responds to stimuli coming from a temperature sensor located elsewhere on the channel, or both has remained unclear. Earlier studies showed that Ct deletion abrogates $K_{2P}2.1$ (TREK-1) temperature sensitivity (Maingret *et al*, 2000), a result that could suggest that the intracellular domain contains temperature-sensing elements. However, the same deletion showed decreased basal activity (Patel *et al*, 1998) and insensitivity to activation by chemical agonists and mechanical force (Maingret *et al*, 1999), raising the possibility that the loss of temperature sensitivity arose from a global effect rather than by loss of an actual temperature sensor. We used the $K_{2P}2.1$-3G and $K_{2P}2.1$-3A mutants that uncouple Ct from the pore to revisit the importance of Ct for $K_{2P}2.1$ (TREK-1) temperature sensitivity. Both $K_{2P}2.1$-3G and $K_{2P}2.1$-3A showed only minimal temperature sensitivity (Figure 6B–D) (I_{40}/I_{14} = 5.73 ± 0.11 and 3.37 ± 0.58, respectively) that was comparable to that of the temperature-insensitive K_{2P} channels from the TASK group (Bagriantsev *et al*, 2011). This blunted response stands in stark contrast to the strong temperature response of WT $K_{2P}2.1$ (TREK-1) (I_{40}/I_{14} mean ± s.e. = 22.71 ± 1.40) (Figure 6D). These clear differences strongly support the original idea that Ct is an important element of the temperature response (Maingret *et al*, 2000) and further indicate that the pore domain itself lacks a substantial temperature response.

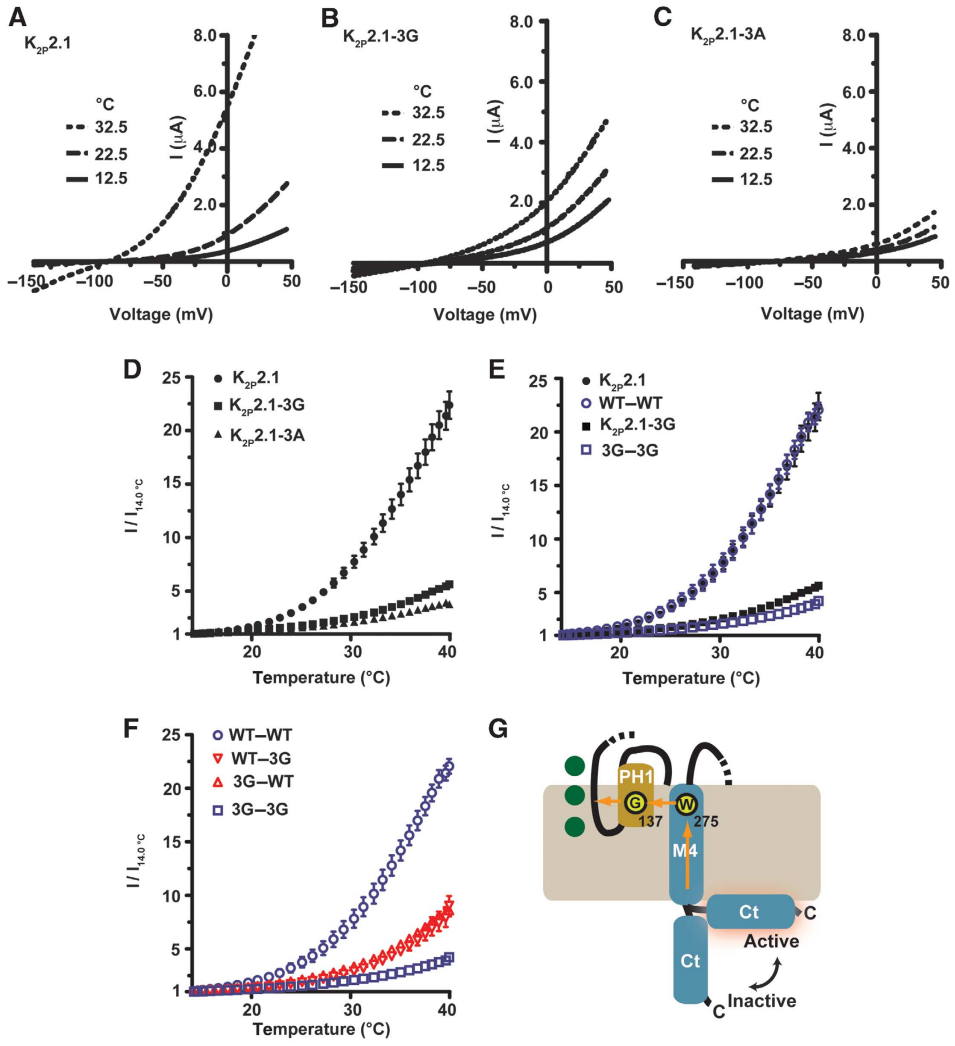

Figure 6 Both C-terminal domains are required for the $K_{2P}2.1$ (TREK-1) temperature response. (**A–C**) Exemplar two-electrode voltage clamp recordings of $K_{2P}2.1$ (TREK-1) (**A**), $K_{2P}2.1$-3G (**B**), and $K_{2P}2.1$-3A (**C**) responses to temperature in 2 mM $[K^+]_o$ pH 7.4. Currents were elicited by a ramp from −150 to +50 mV, from a −80 mV holding potential. (**D–F**) Quantification of the temperature responses. Data (mean ± s.e., $n \geqslant 6$, $N \geqslant 2$) was taken at 0 mV and normalized to channel activity at 14°C. (**G**) Cartoon model of how Ct couples to the C-type gate of $K_{2P}2.1$ (TREK-1). M4, transmembrane segment 4. Channel elements come from a single subunit. Transmembrane segments M1–M3 and pore helix 2 are not depicted. Dashed regions indicate connections to parts of the subunit that are not shown. Green circles represent potassium ions in the selectivity filter.

Given the clear importance of Ct for temperature responses, we next asked whether the two Ct domains present in a mature $K_{2P}2.1$ (TREK-1) are required to control temperature responses by examining the temperature responses of tandem $K_{2P}2.1$ (TREK-1) channels. WT–WT showed a temperature response that was indistinguishable from unlinked $K_{2P}2.1$ (TREK-1) ($I_{40}/I_{14} = 22.34 \pm 0.68$, 22.71 ± 1.40, $P = 0.89$, *t*-test for WT-WT and $K_{2P}2.1$, respectively) (Figure 6E). Notably, use of a shorter linker, 10 amino acids rather than 20, resulted in channels having a temperature sensitivity that was increased relative to unlinked $K_{2P}2.1$ (TREK-1) (Supplementary Figure S5C), a result that further supports the idea that Ct is critical for temperature sensing. Uncoupling both Cts from the pore domain of the tandem, 3G–3G, yielded a channel that lacked a robust temperature response ($I_{40}/I_{14} = 4.67 \pm 0.21$) and that matched the response of the unlinked $K_{2P}2.1$-3G (Figure 6E). Strikingly, channels having the decoupling mutation on only one subunit, 3G–WT and WT–3G, were only moderately sensitive to temperature ($I_{40}/I_{14} = 9.06 \pm 0.67$ and 9.97 ± 0.76, respectively; $P = 0.4$, Student's *t*-test) (Figure 6F). These results indicate that both Ct domains are required to achieve full temperature response. Taken together, our results support the idea that the temperature sensor is confined within the C-terminal domain of $K_{2P}2.1$ (TREK-1) (Maingret *et al*, 2000), while the C-type gate lacks robust sensitivity to heat.

Discussion

$K_{2P}2.1$ (TREK-1) belongs to a unique subgroup of two-pore potassium channels characterized by the ability to integrate different types of regulatory cues that range from acidosis, to metabolic signalling cascades, to physical inputs such as heat and mechanical force (Honore, 2007; Enyedi and Czirjak, 2010). Previous studies have identified a number of sensory regions located in different parts of the channel that endow it with the ability to respond to these diverse regulatory cues. With the exception of extracellular pH, which is sensed by a

histidine residue in the extracellular P1 loop (Cohen *et al*, 2008), all other sensor elements are found in the cytoplasmic C-terminal domain, Ct. These include the intracellular pH sensor Glu306 (Honore *et al*, 2002), a cluster of positively charged amino acids that modulate interaction with phospholipids (Chemin *et al*, 2005; Lopes *et al*, 2005; Chemin *et al*, 2007), and a number of phosphorylation sites, including Ser300 and Ser333 (Patel *et al*, 1998; Murbartian *et al*, 2005). Results from several groups have established that the response of K_{2P}2.1 (TREK-1) to extracellular pH (Cohen *et al*, 2008; Sandoz *et al*, 2009; Bagriantsev *et al*, 2011; Ma *et al*, 2011), intracellular pH (Piechotta *et al*, 2011), temperature, and mechanical force (Bagriantsev *et al*, 2011) involves the engagement of a selectivity filter-based C-type gate that is sensitive to the concentration of extracellular permeant ions. Given the diverse locations of the sensory elements, which are located on both extracellular and intracellular domains, it has remained unclear how signals that are detected by the various sensors are transmitted to the common C-type gate. This question is brought into sharp relief by the fact that the major sensory element, Ct, is located on the opposite side of the membrane from the selectivity filter.

A number of lines of evidence presented here indicate that there is substantial crosstalk between Ct and the C-type gate. First, experiments examining the response of K_{2P}2.1 (TREK-1) to modulation by sustained changes in membrane potential, which are linked to the effect of signal transduction cascades on Ct (Cohen and Zilberberg, 2006; Segal-Hayoun *et al*, 2010), show a blunting of the response by $[K^+]_O$ that is similar to the effect of the loss of a target phosphorylation site (Figure 1D and E). Second, decoupling Ct from the pore by replacement of residues at the M4–Ct junction eliminates both Ct-dependent modulation by membrane potential (Figure 4B and C) and the majority of the temperature-dependent behaviour of the channel (Figure 6D) in accord with the proposed central role of Ct in temperature sensing (Maingret *et al*, 2000). Third, activation of the channel by the Ct mutant E306A stabilizes the C-type gate to closure by extracellular pH (Figure 4E) and this effect is reversed by combination of E306A with the Ct decoupling triple glycine mutant (Figure 4F). Taken together with the prior findings that activatory mutations in the C-type gate blunt the response to temperature and stretch (Bagriantsev *et al*, 2011), these new studies strongly support a model in which the status of Ct is directly transmitted to the pore.

Based on functional data, Chemin *et al* (2005) hypothesized that Ct-mediated K_{2P}2.1 (TREK-1) activation is accompanied by association between Ct and the plasma membrane inner leaflet, whereas dissociation from the membrane accompanies inhibition. Direct optical measurements of Ct–plasma membrane interactions provided strong support for this hypothesis (Sandoz *et al*, 2011). Together, these findings suggested that Ct undergoes conformation changes in response to regulatory commands. How such changes might be transmitted to the C-type gate remained an open question. Building on the prior identification of the activating M4 mutant W275S (Bagriantsev *et al*, 2011), which is likely to interact with elements of the pore, we identified a position in PH1, Gly137, that is centrally involved in the function of the C-type gate (Figure 2). Changing this residue, which is largely conserved in the K_{2P} family as a small sidechain (Supplementary Figure S2), to a larger residue that is found in members of the TASK K_{2P} subfamily, G137I, stabilizes a potassium-selective conformation of the selectivity filter (Supplementary Figure S3) and renders K_{2P}2.1 (TREK-1) irresponsive to both extracellular (Figure 2C and D) and intracellular (Figure 3C and D) gating commands. These results identify PH1 as a crucial element of the selectivity filter gate, and are concordant with the role of pore helices in selectivity filter-based gating in other ion channels (Yang *et al*, 1997; Alagem *et al*, 2003; Cordero-Morales *et al*, 2006; Tao *et al*, 2009; Cheng *et al*, 2011; Cordero-Morales *et al*, 2011b; Chatelain *et al*, 2012). Moreover, this role appears general for K_{2P}s as the converse change, I88G, causes both K_{2P}3.1 (TASK-1) and K_{2P}9.1 (TASK-3) to become more sensitive to pH_o-induced closure (Figure 2E-J). Analysis of the recently determined structure of K_{2P}4.1 (*KCNK4*/TRAAK) (Brohawn *et al*, 2012), a K_{2P}2.1 (TREK-1) relative, indicates the positions of Gly137 and Trp275, which are conserved between K_{2P}2.1 (TREK-1) and K_{2P}4.1 (TRAAK), abut each other (Figure 3E). This physical proximity provides a mechanistic rationale for how changes at either position impact the function of the C-type gate and indicates a clear link between transmembrane helix M4 position Trp275, which is crucial for C-type gating of many K_{2P} channels (Bagriantsev *et al*, 2011; Chatelain *et al*, 2012) and the C-type gate.

The observations that channel activation by the E306A Ct mutant reduces sensitivity to pH_o-induced channel closure and that this effect is suppressed by the presence of the M4–Ct junction triple glycine change strongly suggests that Ct acts on M4. Examination of the effects of these mutants in the context of tandem K_{2P}2.1 (TREK-1) channels further demonstrates that the effects of Ct activation are transmitted through M4 by a *cis*-type mechanism (Figure 5D). Together, these findings lead us to propose a model in which the status of Ct is directly conveyed to the pore through M4 and the Gly137–Trp275 junction (Figure 6G). Such a connection not only explains how Ct can influence the pore but also fits with the findings that stabilization of the C-type gate by external permeant ions (Figure 1D and (Bagriantsev *et al*, 2011)) or an M4 mutant that stabilizes the potassium-selective conformation of the filter, W275S (Bagriantsev *et al*, 2011), renders the channel irresponsive to commands from the intracellular Ct-resident sensors.

In other potassium channel classes, activation involves a widening of the intracellular aperture, known as the lower gate, formed by the pore-lining helices. This conformational change is driven by movement of the voltage sensor domains in K_vs (Long *et al*, 2005; Tombola *et al*, 2006) or the intracellular domains in bacterial (Clarke *et al*, 2010; Bavro *et al*, 2012) and mammalian (Hansen *et al*, 2011; Whorton and MacKinnon, 2011) inward rectifiers and the bacterial channel KcsA (Uysal *et al*, 2009). The finding that the K_{2P} M4 pore-lining helix, which is attached to an interacellular sensor domain, Ct, that is thought to move to the membrane upon activation, plays a key role in K_{2P} gating would seem to fit this generalized paradigm, particularly as mammalian inward rectifier activation involves the association of the intracellular domains with the membrane and phosphoinositide lipids (Rohacs *et al*, 1999; Zhang *et al*, 1999; Logothetis *et al*, 2007; Hansen *et al*, 2011; Whorton and MacKinnon, 2011). However, whereas opening of the lower

gate in other potassium channel classes starts ion flow that eventually leads to slow closure of the selectivity filter by C-type inactivation (Cuello *et al*, 2010a,b; McCoy and Nimigean, 2012), both functional (Zilberberg *et al*, 2001; Cohen *et al*, 2008; Bagriantsev *et al*, 2011; Piechotta *et al*, 2011) and structural (Brohawn *et al*, 2012; Miller and Long, 2012) data suggest that the K_{2P} lower gate is open independent of channel stimulation and that, instead, the main gating events occur at the selectivity filter C-type-like gate. Thus, although structural changes driven by movement of the Ct domain may cause twisting and rotational changes to the pore-lining helices similar to those seen in other potassium channel types, changes in the K_{2P} M4 segment should have a major effect only at the selectivity filter. Such a connection seems plausible given that the movement of the *Drosophila melanogaster* K_{2P} KCNK0 (Ben-Abu *et al*, 2009) inner gate region has been shown to affect conformation of the selectivity filter gate and that coupling between the cytoplasmic domain and selectivity filter have been observed in other potassium channels (Clarke *et al*, 2010; Cuello *et al*, 2010a; Bavro *et al*, 2012). In addition, the asymmetric nature of the K_{2P} pore may require substantial variation from the paradigm drawn from the better structurally characterized symmetric Kv and inward rectifier channels. Delineating these differences will require the determination of K_{2P} channel structures that represent different states along the activation pathway.

One of the interesting properties of K_{2P}2.1 (TREK-1) is that it is activated by temperature (Maingret *et al*, 2000), a trait that appears to be important for the temperature sensitivity of nerve C-fibres (Alloui *et al*, 2006) and temperature preference in mice (Alloui *et al*, 2006; Noel *et al*, 2009). Our studies indicate that Ct serves as the major temperature-sensing element (Figure 6D and E) and are consistent with prior suggestions made from studies of truncation mutants (Maingret *et al*, 2000). The observation that disrupting the structure between M4 and Ct significantly reduces the temperature response strongly suggests that K_{2P}2.1 (TREK-1) contains a discrete temperature sensor in Ct that gates a largely temperature-insensitive pore module. Further, our studies with tandem channels here suggest that both Cts are necessary to elicit full temperature response (Figure 6F).

How heat-sensitive ion channels open in response to temperature changes remains an intensely researched question. The paradigm of temperature-sensitivity outlined here for K_{2P}2.1 (TREK-1) may have general relevance for the operation of other temperature-sensitive ion channels such as those from the transient receptor potential (TRP) family (Caterina *et al*, 1997; Peier *et al*, 2002; Hamada *et al*, 2008; Gracheva *et al*, 2010). Indeed, multiple studies suggest that even though the TRP channel's selectivity filter domain is a necessary component of temperature activation pathway (Grandl *et al*, 2008; Myers *et al*, 2008; Grandl *et al*, 2010; Yang *et al*, 2010; Cui *et al*, 2012), the thermosensory regions appear to reside in the intracellular domains (Cordero-Morales *et al*, 2011a; Gracheva *et al*, 2011; Yao *et al*, 2011; Zhong *et al*, 2012). Thus, even though an increase in temperature is likely to produce conformational changes throughout the channel, the available data suggest that some domains may be more labile to temperature changes than others, and serve as authentic temperature sensors.

The data presented here show that intracellular Ct mediates K_{2P}2.1 (TREK-1) response to a wide range of signals by controlling the extracellular C-type gate. This coupling further supports the idea that diverse inputs sensed by different parts of the channel converge on a single gate (Bagriantsev *et al*, 2011) and suggests that the polymodal gating mechanism of K_{2P}2.1 (TREK-1) has evolved through coupling of various molecular sensors to a common gating apparatus.

Materials and methods

Molecular biology

Standard molecular biology techniques were used throughout. For expression in oocytes, murine K_{2P} channels cloned into pGEMHE/pMO vector (Bagriantsev *et al*, 2011) were used. To construct K_{2P}2.1 (TREK-1) tandems, open reading frames for individual subunits were connected with a linker encoding the AAAGSGGSGGSGGSSG SSGS sequence and cloned into pGEMHE vector. The first subunit was N-terminally tagged with a HA sequence: YPYDVPDYA. Each clone was verified by DNA sequencing.

Electrophysiology

Recordings were performed from defolliculated stage V–VI *Xenopus* oocytes 24–72 h after injection with 0.015–10.0 ng cRNA, using microelectrodes (0.3–3.0 MΩ) filled with 3 M KCl. Data were acquired using the GeneClamp 500B (MDS Analytical Technologies) amplifier controlled by the pClamp software (Molecular Devices), and digitized at 1 kHz using Digidata 1332A (MDS Analytical Technologies). Recording solutions, 2 K (96 mM NaCl, 2 mM KCl, 1.8 mM $CaCl_2$, and 2.0 mM $MgCl_2$) and 90 K (90 mM KCl, 8 mM NaCl, 1.8 mM $CaCl_2$, and 2.0 mM $MgCl_2$), were buffered with 10 mM Tris (pH 9.0, 8.1), 5 mM HEPES (pH 7.8, 7.4, 7.1), or 5 mM MES (pH 6.5, 5.9). To measure the effect of membrane potential (E_m) on K_{2P}2.1 (TREK-1) activity, currents were evoked from − 100 or 0 mV holding potential every 15 s with a 300-ms-long ramp from − 150 to 50 mV (22.5°C). For pH_o experiments, currents were evoked from a − 80 or 0 mV holding potential (for 2 and 90 K solutions, respectively) with a 1-s-long ramp from − 150 to + 50 mV. The solutions with different pH were exchanged at 22.5°C consecutively from pH 9.0 to pH 5.9. For oocyte batches showing high background currents at pH ≤ 6.5, NaCl and KCl were substituted with equimolar amounts of Na- or K-gluconate. Data were fitted with a modified Hill's equation: $I = I_{min} + (I_{max} - I_{min})/(1 + 10\text{^}((pH_oIC_{50} - pH_o)*H))$, where I_{max} and I_{min} are maximal and minimal current values, respectively, pH_oIC_{50} is a half-maximal effective pH_o value, and H is the Hill coefficient. For temperature experiment, recording solutions were heated using the SC-20 in-line heater–cooler combined with LCS-1 liquid cooling system operated by the CL-100 bipolar temperature controller (Warner Instruments). Temperature readings were taken in the recording chamber using a CL-100-controlled thermistor placed 1 mm away from the oocyte. Currents were evoked from a − 80 mV holding potential with a 300-ms-long ramp from − 150 to + 50 mV.

Immunoblot analysis

Oocytes were injected with 0.5 ng cRNA and lyzed after 48 h by repetitive pipetting in a cold buffer of 150 mM NaCl, 1.06 mM KH_2PO_4, 2.07 mM Na_2HPO_4, 1% Triton X100, pH7.4 supplemented with antiproteases. Following a 30-min incubation on ice, crude lysates were clarified by centrifugation for 15 min at 20 000 *g* (4°C) and incubated for 30 min at 4°C or at room temperature with or without endoglycosydase H (New England Biolabs). Lysates were treated for 30 min at 50°C with a sample buffer containing 2% SDS and 2% β-mercaptoethanol, and analysed by immunoblotting with the HA7 anti-HA antibodies (Sigma).

Supplementary data

Supplementary data are available at *The EMBO Journal* Online (http://www.embojournal.org).

Acknowledgements

This work was supported by grants to DLM from NIH R01-MH093603 and the American Heart Association 0740019N, and to SNB from the Life Sciences Research Foundation. We thank E Gracheva, D Julius, and G Thiel for comments on the manuscript. DLM is an AHA Established Investigator. SNB is a Genentech Fellow of the Life Sciences Research Foundation.

Author contributions: DLM and SNB conceived the study. SNB and KAC performed the experiments and analysed the data. DLM analysed the data, and provided guidance and support throughout. DLM and SNB wrote the paper.

Conflict of interest

The authors declare that they have no conflict of interest.

References

Alagem N, Yesylevskyy S, Reuveny E (2003) The pore helix is involved in stabilizing the open state of inwardly rectifying K+ channels. *Biophys J* **85:** 300–312

Alloui A, Zimmermann K, Mamet J, Duprat F, Noel J, Chemin J, Guy N, Blondeau N, Voilley N, Rubat-Coudert C, Borsotto M, Romey G, Heurteaux C, Reeh P, Eschalier A, Lazdunski M (2006) TREK-1, a K+ channel involved in polymodal pain perception. *Embo J* **25:** 2368–2376

Arias JM, Murbartian J, Vitko I, Lee JH, Perez-Reyes E (2005) Transfer of beta subunit regulation from high to low voltage-gated Ca2+ channels. *FEBS Lett* **579:** 3907–3912

Bagriantsev SN, Peyronnet R, Clark KA, Honore E, Minor Jr DL (2011) Multiple modalities converge on a common gate to control K2P channel function. *EMBO J* **30:** 3594–3606

Bavro VN, De Zorzi R, Schmidt MR, Muniz JR, Zubcevic L, Sansom MS, Venien-Bryan C, Tucker SJ (2012) Structure of a KirBac potassium channel with an open bundle crossing indicates a mechanism of channel gating. *Nat Struct Mol Biol* **19:** 158–163

Ben-Abu Y, Zhou Y, Zilberberg N, Yifrach O (2009) Inverse coupling in leak and voltage-activated K+ channel gates underlies distinct roles in electrical signaling. *Nat Struct Mol Biol* **16:** 71–79

Brohawn SG, del Marmol J, MacKinnon R (2012) Crystal structure of the human K2P TRAAK, a lipid- and mechano-sensitive K+ ion channel. *Science* **335:** 436–441

Caterina MJ, Schumacher MA, Tominaga M, Rosen TA, Levine JD, Julius D (1997) The capsaicin receptor: a heat-activated ion channel in the pain pathway. *Nature* **389:** 816–824

Chatelain FC, Bichet D, Douguet D, Feliciangeli S, Bendahhou S, Reichold M, Warth R, Barhanin J, Lesage F (2012) TWIK1, a unique background channel with variable ion selectivity. *Proc Natl Acad Sci USA* **109:** 5499–5504

Chemin J, Patel AJ, Duprat F, Lauritzen I, Lazdunski M, Honore E (2005) A phospholipid sensor controls mechanogating of the K+ channel TREK-1. *EMBO J* **24:** 44–53

Chemin J, Patel AJ, Duprat F, Sachs F, Lazdunski M, Honore E (2007) Up- and down-regulation of the mechano-gated K(2P) channel TREK-1 by PIP (2) and other membrane phospholipids. *Pflugers Arch* **455:** 97–103

Cheng WW, McCoy JG, Thompson AN, Nichols CG, Nimigean CM (2011) Mechanism for selectivity-inactivation coupling in KcsA potassium channels. *Proc Natl Acad Sci USA* **108:** 5272–5277

Clarke CE, Veale EL, Wyse K, Vandenberg JI, Mathie A (2008) The M1P1 loop of TASK3 K2P channels apposes the selectivity filter and influences channel function. *J Biol Chem* **283:** 16985–16992

Clarke OB, Caputo AT, Hill AP, Vandenberg JI, Smith BJ, Gulbis JM (2010) Domain reorientation and rotation of an intracellular assembly regulate conduction in Kir potassium channels. *Cell* **141:** 1018–1029

Cohen A, Ben-Abu Y, Hen S, Zilberberg N (2008) A novel mechanism for human K2P2.1 channel gating. Facilitation of C-type gating by protonation of extracellular histidine residues. *J Biol Chem* **283:** 19448–19455

Cohen A, Zilberberg N (2006) Fluctuations in Xenopus oocytes protein phosphorylation levels during two-electrode voltage clamp measurements. *J Neurosci Methods* **153:** 62–70

Cordero-Morales JF, Cuello LG, Zhao Y, Jogini V, Cortes DM, Roux B, Perozo E (2006) Molecular determinants of gating at the potassium-channel selectivity filter. *Nat Struct Mol Biol* **13:** 311–318

Cordero-Morales JF, Gracheva EO, Julius D (2011a) Cytoplasmic ankyrin repeats of transient receptor potential A1 (TRPA1) dictate sensitivity to thermal and chemical stimuli. *Proc Natl Acad Sci USA* **108:** E1184–E1191

Cordero-Morales JF, Jogini V, Chakrapani S, Perozo E (2011b) A multipoint hydrogen-bond network underlying KcsA C-type inactivation. *Biophys J* **100:** 2387–2393

Cuello LG, Jogini V, Cortes DM, Pan AC, Gagnon DG, Dalmas O, Cordero-Morales JF, Chakrapani S, Roux B, Perozo E (2010a) Structural basis for the coupling between activation and inactivation gates in K(+) channels. *Nature* **466:** 272–275

Cuello LG, Jogini V, Cortes DM, Perozo E (2010b) Structural mechanism of C-type inactivation in K(+) channels. *Nature* **466:** 203–208

Cui Y, Yang F, Cao X, Yarov-Yarovoy V, Wang K, Zheng J (2012) Selective disruption of high sensitivity heat activation but not capsaicin activation of TRPV1 channels by pore turret mutations. *J Gen Physiol* **139:** 273–283

Enyedi P, Czirjak G (2010) Molecular background of leak K+ currents: two-pore domain potassium channels. *Physiol Rev* **90:** 559–605

Findeisen F, Minor Jr DL (2009) Disruption of the IS6-AID linker affects voltage-gated calcium channel inactivation and facilitation. *J Gen Physiol* **133:** 327–343

Fink M, Duprat F, Lesage F, Reyes R, Romey G, Heurteaux C, Lazdunski M (1996) Cloning, functional expression and brain localization of a novel unconventional outward rectifier K+ channel. *Embo J* **15:** 6854–6862

Gracheva EO, Cordero-Morales JF, Gonzalez-Carcacia JA, Ingolia NT, Manno C, Aranguren CI, Weissman JS, Julius D (2011) Ganglion-specific splicing of TRPV1 underlies infrared sensation in vampire bats. *Nature* **476:** 88–91

Gracheva EO, Ingolia NT, Kelly YM, Cordero-Morales JF, Hollopeter G, Chesler AT, Sanchez EE, Perez JC, Weissman JS, Julius D (2010) Molecular basis of infrared detection by snakes. *Nature* **464:** 1006–1011

Grandl J, Hu H, Bandell M, Bursulaya B, Schmidt M, Petrus M, Patapoutian A (2008) Pore region of TRPV3 ion channel is specifically required for heat activation. *Nat Neurosci* **11:** 1007–1013

Grandl J, Kim SE, Uzzell V, Bursulaya B, Petrus M, Bandell M, Patapoutian A (2010) Temperature-induced opening of TRPV1 ion channel is stabilized by the pore domain. *Nat Neurosci* **13:** 708–714

Hamada FN, Rosenzweig M, Kang K, Pulver SR, Ghezzi A, Jegla TJ, Garrity PA (2008) An internal thermal sensor controlling temperature preference in Drosophila. *Nature* **454:** 217–220

Hansen SB, Tao X, MacKinnon R (2011) Structural basis of PIP2 activation of the classical inward rectifier K+ channel Kir2.2. *Nature* **477:** 495–498

Honore E (2007) The neuronal background K2P channels: focus on TREK1. *Nat Rev Neurosci* **8:** 251–261

Honore E, Maingret F, Lazdunski M, Patel AJ (2002) An intracellular proton sensor commands lipid- and mechano-gating of the K(+) channel TREK-1. *Embo J* **21:** 2968–2976

Logothetis DE, Jin T, Lupyan D, Rosenhouse-Dantsker A (2007) Phosphoinositide-mediated gating of inwardly rectifying K(+) channels. *Pflugers Arch* **455:** 83–95

Long SB, Campbell EB, Mackinnon R (2005) Voltage sensor of Kv1.2: structural basis of electromechanical coupling. *Science* **309:** 903–908

Lopes CM, Gallagher PG, Buck ME, Butler MH, Goldstein SA (2000) Proton block and voltage gating are potassium-dependent in the cardiac leak channel Kcnk3. *J Biol Chem* **275:** 16969–16978

Lopes CM, Rohacs T, Czirjak G, Balla T, Enyedi P, Logothetis DE (2005) PIP2 hydrolysis underlies agonist-induced inhibition and regulates voltage gating of two-pore domain K+ channels. *J Physiol* **564:** 117–129

Ma XY, Yu JM, Zhang SZ, Liu XY, Wu BH, Wei XL, Yan JQ, Sun HL, Yan HT, Zheng JQ (2011) External Ba2+ block of the two-pore domain potassium channel TREK-1 defines conformational transition in its selectivity filter. *J Biol Chem* **286:** 39813–39822

Maingret F, Lauritzen I, Patel AJ, Heurteaux C, Reyes R, Lesage F, Lazdunski M, Honore E (2000) TREK-1 is a heat-activated background K(+) channel. *Embo J* **19:** 2483–2491

Maingret F, Patel AJ, Lesage F, Lazdunski M, Honore E (1999) Mechano- or acid stimulation, two interactive modes of activation of the TREK-1 potassium channel. *J Biol Chem* **274:** 26691–26696

McCoy JG, Nimigean CM (2012) Structural correlates of selectivity and inactivation in potassium channels. *Biochim Biophys Acta* **1818:** 272–285

Miller AN, Long SB (2012) Crystal structure of the human two-pore domain potassium channel K2P1. *Science* **335:** 432–436

Murbartian J, Lei Q, Sando JJ, Bayliss DA (2005) Sequential phosphorylation mediates receptor- and kinase-induced inhibition of TREK-1 background potassium channels. *J Biol Chem* **280:** 30175–30184

Myers BR, Bohlen CJ, Julius D (2008) A yeast genetic screen reveals a critical role for the pore helix domain in TRP channel gating. *Neuron* **58:** 362–373

Niemeyer MI, Cid LP, Pena-Munzenmayer G, Sepulveda FV (2010) Separate gating mechanisms mediate the regulation of K2P potassium channel TASK-2 by intra- and extracellular pH. *J Biol Chem* **285:** 16467–16475

Noel J, Sandoz G, Lesage F (2011) Molecular regulations governing TREK and TRAAK channel functions. *Channels (Austin)* **5:** 402–409

Noel J, Zimmermann K, Busserolles J, Deval E, Alloui A, Diochot S, Guy N, Borsotto M, Reeh P, Eschalier A, Lazdunski M (2009) The mechano-activated K+ channels TRAAK and TREK-1 control both warm and cold perception. *Embo J* **28:** 1308–1318

Patel AJ, Honore E, Maingret F, Lesage F, Fink M, Duprat F, Lazdunski M (1998) A mammalian two pore domain mechano-gated S-like K+ channel. *Embo J* **17:** 4283–4290

Peier AM, Reeve AJ, Andersson DA, Moqrich A, Earley TJ, Hergarden AC, Story GM, Colley S, Hogenesch JB, McIntyre P, Bevan S, Patapoutian A (2002) A heat-sensitive TRP channel expressed in keratinocytes. *Science* **296:** 2046–2049

Piechotta PL, Rapedius M, Stansfeld PJ, Bollepalli MK, Ehrlich G, Andres-Enguix I, Fritzenschaft H, Decher N, Sansom MS, Tucker SJ, Baukrowitz T (2011) The pore structure and gating mechanism of K2P channels. *EMBO J* **30:** 3607–3619

Rohacs T, Chen J, Prestwich GD, Logothetis DE (1999) Distinct specificities of inwardly rectifying K(+) channels for phosphoinositides. *J Biol Chem* **274:** 36065–36072

Sandoz G, Bell SC, Isacoff EY (2011) Optical probing of a dynamic membrane interaction that regulates the TREK1 channel. *Proc Natl Acad Sci USA* **108:** 2605–2610

Sandoz G, Douguet D, Chatelain F, Lazdunski M, Lesage F (2009) Extracellular acidification exerts opposite actions on TREK1 and TREK2 potassium channels via a single conserved histidine residue. *Proc Natl Acad Sci USA* **106:** 14628–14633

Sandoz G, Tardy MP, Thummler S, Feliciangeli S, Lazdunski M, Lesage F (2008) Mtap2 is a constituent of the protein network that regulates twik-related K+ channel expression and trafficking. *J Neurosci* **28:** 8545–8552

Sandoz G, Thummler S, Duprat F, Feliciangeli S, Vinh J, Escoubas P, Guy N, Lazdunski M, Lesage F (2006) AKAP150, a switch to convert mechano-, pH- and arachidonic acid-sensitive TREK K(+) channels into open leak channels. *EMBO J* **25:** 5864–5872

Segal-Hayoun Y, Cohen A, Zilberberg N (2010) Molecular mechanisms underlying membrane-potential-mediated regulation of neuronal K2P2.1 channels. *Mol Cell Neurosci* **43:** 117–126

Talley EM, Solorzano G, Lei Q, Kim D, Bayliss DA (2001) CNS distribution of members of the two-pore-domain (KCNK) potassium channel family. *J Neurosci* **21:** 7491–7505

Tao X, Avalos JL, Chen J, MacKinnon R (2009) Crystal structure of the eukaryotic strong inward-rectifier K+ channel Kir2.2 at 3.1 A resolution. *Science* **326:** 1668–1674

Tombola F, Pathak MM, Isacoff EY (2006) How does voltage open an ion channel? *Annu Rev Cell Dev Biol* **22:** 23–52

Uysal S, Vasquez V, Tereshko V, Esaki K, Fellouse FA, Sidhu SS, Koide S, Perozo E, Kossiakoff A (2009) Crystal structure of full-length KcsA in its closed conformation. *Proc Natl Acad Sci USA* **106:** 6644–6649

Whorton MR, MacKinnon R (2011) Crystal structure of the mammalian GIRK2 K+ channel and gating regulation by G proteins, PIP2, and sodium. *Cell* **147:** 199–208

Yamamoto Y, Hatakeyama T, Taniguchi K (2009) Immunohistochemical colocalization of TREK-1, TREK-2 and TRAAK with TRP channels in the trigeminal ganglion cells. *Neurosci Lett* **454:** 129–133

Yang F, Cui Y, Wang K, Zheng J (2010) Thermosensitive TRP channel pore turret is part of the temperature activation pathway. *Proc Natl Acad Sci USA* **107:** 7083–7088

Yang J, Yu M, Jan YN, Jan LY (1997) Stabilization of ion selectivity filter by pore loop ion pairs in an inwardly rectifying potassium channel. *Proc Natl Acad Sci USA* **94:** 1568–1572

Yao J, Liu B, Qin F (2011) Modular thermal sensors in temperature-gated transient receptor potential (TRP) channels. *Proc Natl Acad Sci USA* **108:** 11109–11114

Zhang H, He C, Yan X, Mirshahi T, Logothetis DE (1999) Activation of inwardly rectifying K+ channels by distinct PtdIns(4,5)P2 interactions. *Nat Cell Biol* **1:** 183–188

Zhang Y, Chen YH, Bangaru SD, He L, Abele K, Tanabe S, Kozasa T, Yang J (2008) Origin of the voltage dependence of G-protein regulation of P/Q-type Ca2+ channels. *J Neurosci* **28:** 14176–14188

Zhong L, Bellemer A, Yan H, Honjo K, Robertson J, Hwang RY, Pitt GS, Tracey WD (2012) Thermosensory and non-thermosensory isoforms of Drosophila melanogaster TRPA1 reveal heat sensor domains of a thermoTRP channel. *Cell Rep* **1:** 43–55

Zilberberg N, Ilan N, Goldstein SA (2001) KCNKO: opening and closing the 2-P-domain potassium leak channel entails "C-type" gating of the outer pore. *Neuron* **32:** 635–648

